

## Photochemistry of organic molecules in microscopic reactors

Nicholas J. Turro

Department of Chemistry, Columbia University, New York, New York 10027

**ABSTRACT** The photochemistry of dibenzyl ketone and its derivatives has been employed to investigate the ability of zeolite molecular sieves to modify and to control the reaction channels available to organic molecules adsorbed on the internal and external zeolite surfaces. It is found that the observed photochemistry is very sensitive to the size/shape characteristics of the substrate ketones and of the pores and internal void space of the zeolites. Although unprecedented reactions of ketones have been found to be induced by absorption of the ketones on the zeolite surfaces, the reactions are consistent with expectations based on the topological structure of the zeolite surfaces and on the mechanism of ketone photolysis in homogeneous solution.

### ZEOLITE MOLECULAR SIEVES. DESIGNER MICROSCOPIC REACTORS

Zeolites (from the Greek words *zeo*, "to boil" and *lithos* "stone")<sup>1</sup> are synthetic or natural minerals that often expel water so violently when heated that they appear to boil. Classical zeolites are crystalline aluminosilicates whose internal porous structure contain channels and/or cages filled with exchangeable cations and which may also be filled with adsorbed water. The framework composition of zeolites consists of cations, aluminum, silicon, and oxygen. The framework constitution of zeolites consists of tetrahedral Al atoms and tetrahedral Si atoms linked by the sharing of O atoms (Figure 1). The porous structure of zeo-

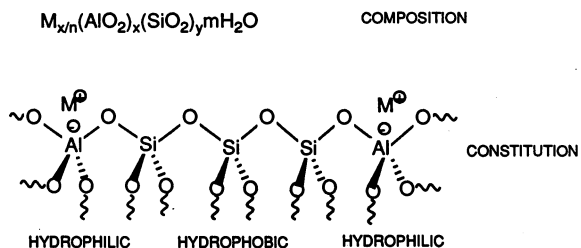


Figure 1. Composition and constitution of a classical aluminosilicate zeolite framework. The subscript *x* refers to the number of Al atoms (negative charges) in the framework; the subscript *y* refers to the number of Si atoms in the framework; and the subscript *n* refers to the charge of cation *M*.

lites results from the framework configuration, i.e., the three-dimensional geometric network of  $AlO_4$  and  $SiO_4$  tetrahedra. The zeolite frameworks which are obtained from natural or synthetic preparations contain pores, channels, cages, and interconnected voids. These void spaces and the internal zeolite surface occur in periodic fashion because of the crystalline nature of the framework. The combination of the topology of the internal void space and the chemical characteristics of the internal framework structure provide chemists with "designer microscopic reactors" in which chemical reactions can be performed. It can be imagined that the size and shape of these microscopic reactors, in conjunction with the peculiarities of molecular diffusion in periodically repeating void spaces will result in unusual characteristics of chemical reactions which are performed on molecules adsorbed on zeolites. Indeed, the ability of zeolites to selectively adsorb molecules based on size/shape selectivity rules has led to their designation as "molecular sieves". As a result of this "sieving" characteristic, the usual domination of substrate molecular structure in determining the course of chemical reactions might be replaced in certain circumstances by a domination of environmental structure in determining the course of chemical reactions for reactions conducted on zeolite molecular sieves. In this report we show how these ideas can be given experimental realization by the judicious selection of zeolites, substrates, and photoreactions. Before describing the actual systems investigated, we shall review briefly some characteristics of important classes of zeolites whose internal surface and internal void space will drive the chemist's imagination in the selection of substrates and photoreactions. Then we shall review a photoreaction whose outstanding generality, mechanistic characteristics, engineering versatility, and convenience of execution and analysis will further define the selection of substrates for study.

## COMPOSITION, CLASSES AND CHARACTERISTICS OF ZEOLITES

### Some structural classes of zeolites. The Pentasils and Faujasites

The composition of classical zeolites consists of  $\text{AlO}_4$  and  $\text{SiO}_4$  tetrahedral building blocks. Each  $\text{AlO}_4$  unit bears a net negative charge (Al is normally trivalent, so the fourth bond to oxygen results in a negative charge on the Al atom) which must be compensated by the presence of cations such as  $\text{H}^+$ ,  $\text{Na}^+$ ,  $\text{Ca}^{+2}$ , etc. The latter are generally mobile, because they are ionically and not covalently bound to the framework structure. Cations may occupy various sites within the framework depending on their size, charge, and degree of hydration. To maintain electrical neutrality there must exist a 1:1 relationship between the Al content of the framework composition and the number of positive charges provided by the mobile cations. This requirement means that the negative charge on the  $\text{AlO}_4$  units indirectly determine the hydrophilicity of the zeolite framework, i.e., the greater the number of Al atoms, the greater the number of cations and sites which are capable of adsorbing water. The ratio of Si atoms to Al atoms (the Si/Al ratio) in zeolites may be varied from about 1 to essentially infinity. The lower limit of 1 is set by the energetic disadvantage of forming  $\text{Al-O-Al}$  units (i.e., the disadvantage of close proximity of negative charges). Thus, in the extreme, zeolites may be strongly hydrophilic (Si/Al ratio small) or strongly hydrophobic (Si/Al ratio large). As might be expected, the Si/Al ratio is also important in determining the details of formation of the crystalline framework structure and, hence, in determining the size, shape, and topological characteristics of the internal void space.

We now consider important families of zeolites that fall near the extremes of the hydrophilic and hydrophobic classes, the faujasites and pentasils, respectively. Both families enjoy an enormous and wide usage in the chemical industry as catalysts. The faujasites, for example, are employed as catalysts in the cracking and reformation of petroleum<sup>3</sup> and the pentasils are employed as catalysts in the conversion of methanol to hydrocarbons such as high grade gasoline.<sup>4</sup>

### Faujasites and Pentasils. The X and ZSM classes of zeolites

Among the most famous and useful members of the faujasite and pentasil families of zeolites are the classes termed X and ZSM, respectively. The general structures of these classes are shown in Figure 2. By convention, the dominant exchangeable cation(s) which appear in the framework is indicated before the name of the class. Hence, NaX designates a X zeolite which contains  $\text{Na}^+$  cations, and NaZSM designates a ZSM zeolite which contains  $\text{Na}^+$  cations. In the figures representing these zeolites, the cations are not shown explicitly (for simplicity and convenience), but their existence must be kept in mind, since the position of cations will be a major factor in determining adsorption sites and diffusional characteristics.

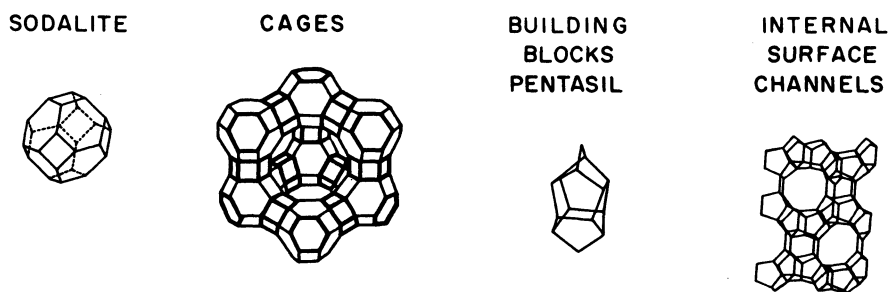


**Figure 2.** Representation of the building blocks and structure of the X (left side) and ZSM (right side) classes of zeolites. The sodalite unit serves as the building block of the faujasite family. The vertices represent Al or Si atoms and the lines represent O bridges. The ratio Si/Al in the X class is about 1.5. At the center of the structure, the window or pore (ca. 8Å diameter) leading to the internal supercage (ca. 13Å) can be seen. The pentasil unit serves as the building block of the ZSM class. In this class the Si/Al ratio is generally high (ca. 20 or greater). The internal structure contains intersecting channels, rather than windows and cages.

In X zeolites the Si and Al tetrahedra are linked together to form a cubooctahedron (Figure 2). In this simple representation the oxygen atoms are not shown explicitly. The Al or Si atoms are located at the vertices of the figure. Thus, the reader must remember that the lines in the figure represent an oxygen bridge. The cubooctahedron is termed the sodalite unit and deserves as the building blocks for the faujasite zeolites. NaX corresponds to the faujasite type with a Si/Al of ca. 1.5, i.e., NaX is a strongly hydrophilic zeolite.

For the chemist, the important topological characteristics (size/shape characteristics of the internal void space) of NaX are the relatively large cavities (roughly spherical "supercages" of ca. 13Å diameter) which are connected by pores (roughly circular "windows" of ca. 8Å diameter). These "supercages" and "windows" constitute the internal surface of NaX zeolites and may be represented topologically as a sequence of periodic "supercages" and "windows" extending in three dimensions. Figure 3 shows a simple representation of a two dimensional

slice of the NaX internal surface. It is important for the chemist to remember that NaX is "loaded" with  $\text{Na}^+$  ions which are not shown explicitly and that individual particles of NaX possess an external surface on which pores exist that provide access to the internal surface only to molecules whose size and shape are such as to allow them to pass readily through these entries to the internal surface, only to molecules whose size and shape are such as to allow them to pass readily through these entries to the internal surface.

The framework of the ZSM class involves a pentasil (Figure 2) rather than a sodalite building block. These building blocks link together to form chains or sheets which generate a void space topology which consists of long tubular channels of diameter of ca.  $6\text{\AA}$  and lengths of ca.  $50\text{\AA}$ . These channels intersect to produce a void network resembling a plumbing pipe network (Figure 4).

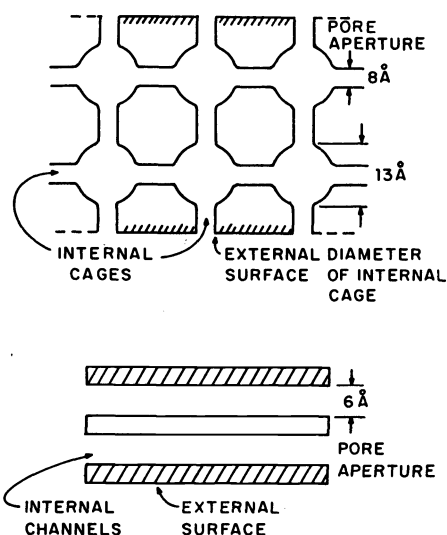


Figure 3. Simple topological representations of the X (top) and ZSM (bottom) classes of zeolites. The representation shows a two dimensional slice of the solid.

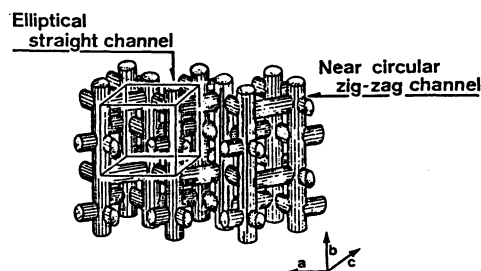


Figure 4. Schematic representation of the void space of the ZSM class of zeolites. Note that there exist two types of channels: the "zig-zag" and linear types. The latter are slightly larger in diameter than the former.

In the systems to be discussed in this report the ratio of the internal surface area to the external surface area will be very large ( $>1000$ ). As a result this large excess of internal relative to external surface will provide a very simple driving force for occupancy of the internal surface for any adsorbed molecules that have the size/shape characteristics which allow entry to the internal surface.

## ZEOLITE MOLECULAR SIEVES IN PHOTOCHEMICAL REACTIONS

### Selection of substrate structure and reaction systems based on zeolite characteristics

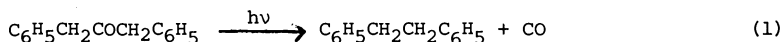
Consideration of the topological features of the zeolite structures shown in Figure 3 provides a powerful driving force to imagine reactions and substrates both to check the validity of the simple representation of zeolite internal framework, and to engineer unusual chemical sequences. The key issues we shall consider are those related to size/shape and diffusion/mobility characteristics of the substrate/zeolite systems.

First, we must select a reaction or family of reactions to study. In photochemistry the Type I (homolytic  $\alpha$ -cleavage)<sup>5</sup> and the Type II (side chain hydrogen abstraction)<sup>6</sup> reactions of ketones are mechanistically well understood, and in many cases, are both experimentally "well-behaved" and convenient from the standpoint of systematic substrate structural variation and product analysis. In this report we consider only the Type I reaction of dibenzyl ketone and related substrates adsorbed on zeolites, although the Type II systems have also been investigated by ourselves<sup>7</sup> and others.<sup>8</sup>

The experimental game plan which will unfold will show how the basic working mechanism of the Type I reaction of dibenzyl ketone for homogeneous solutions can serve to drive ideas and to create experimental systems that will both test the validity of the simple topological representation of zeolite structures and suggest ways to use the unique size/shape characteristics of zeolite frameworks to produce totally new chemistry (that is unprecedented in homogeneous solution) by controlling secondary processes which occur after a common primary photochemical process.

**Type I photoreaction of dibenzyl ketone in homogeneous solution. The working mechanism**

The photolysis of dibenzyl ketone (DBK) in a variety of homogeneous solvents results (eqn. 1) in quantitative decarbonylation and production of 1,2-diphenylethane (DPE).<sup>9,10</sup> The mech-



anism of this reaction has been convincingly defined to follow the pathway shown in Figure 5:

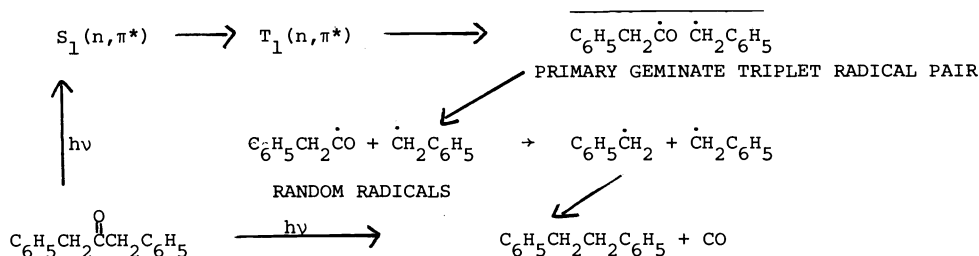


Figure 5. The working mechanism for photolysis of dibenzyl ketone in homogeneous solution.

- (1) Absorption of light produces a  $^1n, \pi^*$  state which crosses with high efficiency to a  $^3n, \pi^*$  state, the site of the primary photochemical processes of homolytic  $\alpha$ -cleavage;
- (2) A geminate, primary triplet radical pair ( $\text{C}_6\text{H}_5\text{CH}_2\dot{\text{C}}\text{O} \dot{\text{C}}\text{H}_2\text{C}_6\text{H}_5$ ) is produced and separates by diffusion to form random radicals;
- (3) The  $\text{C}_6\text{H}_5\text{CH}_2\dot{\text{C}}\text{O}$  species undergoes decarbonylation at a rate<sup>11</sup> of ca.  $10^7\text{s}^{-1}$  to produce  $\text{C}_6\text{H}_5\dot{\text{C}}\text{H}_2$  and CO;
- (4) In a second order process random  $\text{C}_6\text{H}_5\dot{\text{C}}\text{H}_2$  radicals couple to produce DPE.

We note that zeolite structures might be able to impact on the diffusional separation of radical pairs and also on the choice of radical pair reactions available to radical pairs. For example, the zeolite structure might inhibit the diffusional separation of the primary radical pair ( $\text{C}_6\text{H}_5\text{CH}_2\dot{\text{C}}\text{O} \dot{\text{C}}\text{H}_2\text{C}_6\text{H}_5$ ) encouraging previously unprecedented reactions of this radical pair. A second possibility is that the primary geminate radical pair might decarbonylate to produce a secondary geminate radical pair ( $\text{C}_6\text{H}_5\text{CH}_2 \dot{\text{C}}\text{H}_2\text{C}_6\text{H}_5$ ) and high efficiency of secondary geminate pair coupling (as contrasted to random pair coupling) would be encouraged. A third possibility is that the "sieving" characteristics of zeolites might be manifest if an unsymmetrical derivative (ACOB) of DBK is photolyzed. For example, one could envision the two benzyl radicals produced by photolysis (A and B) could be "sieved" as a result of diffusion and different size/shape characteristics of the radical/zeolites and could couple, as a result of the sieving, in a manner that is completely different from that which occurs in homogeneous environments.

Having revealed some of the intriguing qualitative possibilities for employing diffusional characteristics of zeolites to modify the product distributions of Type I reactions, let us now consider how some quantitative characteristics of zeolite structures can drive the selection of specific ketone substrates for investigation.

**Size/shape characteristics of ZSM zeolites**

The ca. 6Å diameter of ZSM channels allows relatively free diffusion of benzene (kinetic diameter ca. 5Å) throughout the internal surface. However, there is a dramatic difference in the rates of diffusion of o-xylene and of p-xylene in ZSM zeolites. The shape of o-xylene is such that there is no orientation (Figure 6) which the molecule can assume and achieve a kinetic diameter of ca 6Å. As a result, o-xylene is kinetically excluded from diffusion into the channels of ZSM zeolites. On the other hand, p-xylene may achieve an orientation in which its long axis lies along the long axis of the ZSM channel, and thereby achieve an effective kinetic diameter (in this orientation) that is equal to that of benzene.

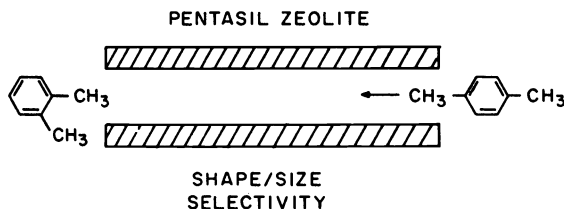
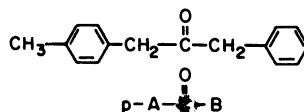
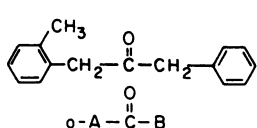


Figure 6. Schematic representation of the shape/size selectivity of pentasil zeolites. The size/shape of p-xylene allows it to be readily adsorbed on the internal zeolite framework, whereas the size/shape of o-xylene prevents it from being readily adsorbed on the internal zeolite framework.

The experimental manifestation of these ideas is the observation that ZSM zeolites serve as chromatographic material to quantitatively separate *o*-xylene from *p*-xylene (the former is not absorbed, and the latter is strongly adsorbed).<sup>2</sup> This striking size/shape selectivity led us to consider DBK derivatives that might display differing photoreactions on zeolites as a result of factors which resemble those that allow the separation of *o*-xylene from *p*-xylene. Our approach was to investigate the photochemistry of the *o*-methyl DBK (*o*-ACOB) and the *p*-methyl DBK (*p*-ACOB) adsorbed on ZSM zeolites.



### Conceptual and experimental strategies for investigation of size/shape selectivity of photoreactions of DBK's adsorbed on ZSM zeolites

The conceptual framework for the investigation of DBK photochemistry on ZSM zeolites involves the production of a geminate triplet radical pair by photolysis of ketones adsorbed on the ZSM surface. From the working mechanism of DBK photochemistry it is expected that the competition between diffusional separation and radical pair reactions will then determine the observed products. From the results of *o*-xylene and *p*-xylene adsorption on ZSM zeolites it is expected that *o*-ACOB will be adsorbed mainly on the external surface of ZSM zeolites, whereas *p*-ACOB will be adsorbed mainly on the internal surface of ZSM zeolites (Figure 7).

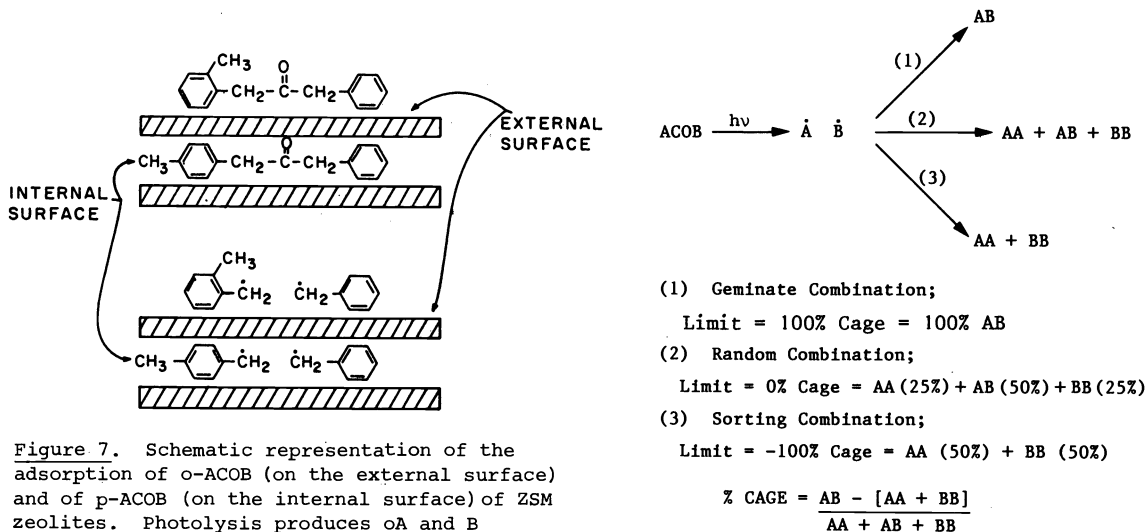


Figure 7. Schematic representation of the adsorption of *o*-ACOB (on the external surface) and of *p*-ACOB (on the internal surface) of ZSM zeolites. Photolysis produces *o*A and B radicals on the external surface, and produces *p*A and B radicals on the internal surface.

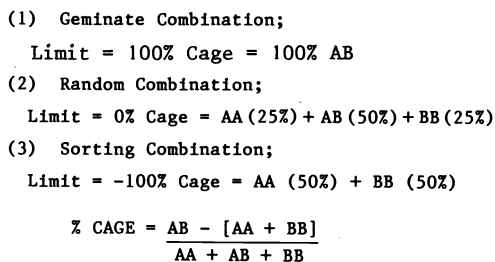
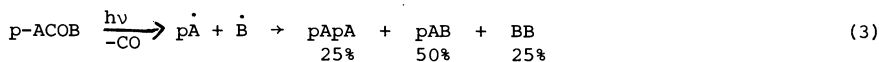
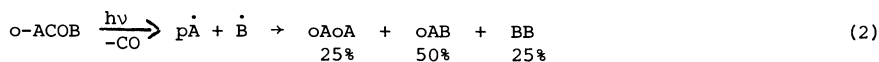


Figure 8. General scheme for possible combinations of radical pairs.

If what happens next is determined by diffusion on the ZSM surface, the reaction pathways available to the radical pairs produced from *o*-ACOB and *p*-ACOB might differ substantially. The experimental strategy is simply to measure product structures and infer how the "reaction channels" are related to the zeolite channels!

The photolysis of *o*-ACOB and *p*-ACOB in homogeneous solution leads to similar results: the three coupling products of benzyl radicals are formed (eqns. 2 and 3):



The ratio of the symmetrical (AA+BB) to asymmetrical (AB) coupling products is 1:1, a result consistent with complete randomization of the initial geminate radical pairs into free radicals. The product distribution can be related quantitatively to the cage effect (i.e., the percent of geminate radical pairs that undergo reaction to form products) as shown by the equation in Figure 8.

Thus, if  $AA+BB=AB$ , the cage effect is 0%; if AB is the only product, the cage effect is 100%. Any situation for which  $AB \neq (AA+BB)$  will result in a value of the cage effect between 0% and 100%. For homogeneous solution,  $AB = (AA+BB)$ , so that the cage effect = 0%. A rather amusing hypothetical situation arises if  $AB < (AA+BB)$ . According to the eqn. for the cage effect (vide supra, Figure 8), in this case the cage effect is negative. In the extreme case, if AA and BB are the only products, the cage effect equals -100%! We shall see that the latter result is actually observed in certain cases, and that the origin of the negative cage effect resides in the unusual size/shape and diffusional characteristics of radicals adsorbed on ZSM surface.

Photolysis of o-ACOB and p-ACOB adsorbed on ZSM zeolites results in strikingly different product distribution (eqns. 4 and 5).<sup>11</sup>



In the case of p-ACOB, the cage effects approach 100%, whereas for o-ACOB, the cage effects approach -100%; i.e., p-ACOB leads to pAB as the major product, whereas o-ACOB leads to oAoA and BB as the major products. We now seek to explain these contrasting results in terms of known size/shape and diffusional characteristics of oA, pA, and B radicals adsorbed on the ZSM surfaces.

### Microscopic interpretation of positive and negative cage effects. Molecular traffic control of chemical reactivity

Analogous to the results of adsorption of o-xylene and p-xylene, we assume that o-ACOB is adsorbed on the external ZSM surface, whereas p-ACOB is adsorbed on the internal ZSM surface. Thus, photolysis produces geminate radical pairs which are initially located on the external surface (oACO B) or on the internal surface (pACO B). From the experimental results, the observed products result from decarbonylation, so that after a time period of the order<sup>12</sup> of  $100 \times 10^{-9}$  after photoexcitation, only oA and B or pA and B occur on the surface.

The observation that pAB is the major product from photolysis of p-ACOB is consistent with the adsorption of this ketone on the internal zeolite framework. The pA B are produced as secondary geminate pairs in a relatively tight fitting channel, so diffusional separation is slow, and coupling to form pAB is efficient. It is also possible that, since diffusion in the ZSM channels is essentially one dimensional, a reduction of dimensionality of diffusion could also contribute to high coupling efficiency.

The observation that oAoA and BB are the major products from photolysis of o-ACOB is consistent with adsorption of this ketone of the external ZSM surface, if the B radicals produced on the external surface are "sieved" into the internal framework faster than they combine with oA radicals. The mechanism proposed in Figure 9 is consistent with the observation of oAoA and BB as major products. Two simple tests of the mechanism are possible: a temperature test and a scavenging test.

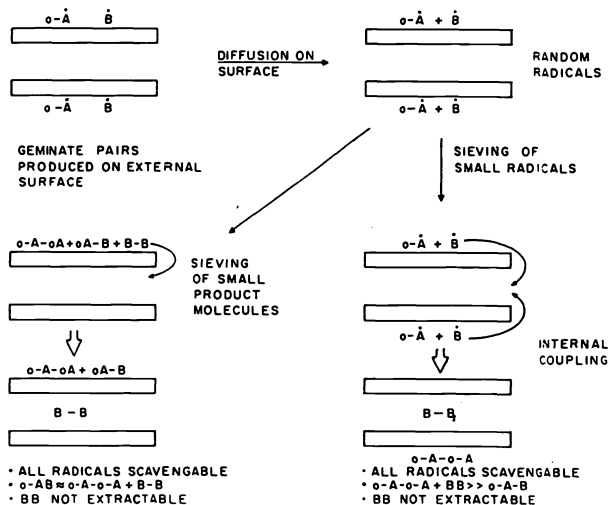


Figure 9. Proposed mechanism for the negative cage effect observed for the photolysis of o-ACOB on ZSM zeolites. See text for discussion.

As the temperature of photolysis is lowered, the major products from photolysis of o-ACOB change from oAoA + BB to a mixture containing ever increasing amounts of oAB. At about  $-20^{\circ}\text{C}$  oAB<sup>2</sup>(oAoA+BB) so that the cage effect has "risen" from ca. -100% to ca. 0%. A further decrease in temperature causes the yield of oAB to continue to increase until at  $-78^{\circ}\text{C}$ , oAB is the major product, i.e., the cage effect is ca. +100%! The temperature effect is consistent with a relatively high activation energy for sieving of B radicals from the external to the internal surface. This causes radical coupling to occur mainly on the external surface as the temperature is decreased to  $-20^{\circ}\text{C}$ . At this temperature random radical coupling occurs on the external surface. Below this temperature, diffusional separation of geminate pairs on the external surface slows down and geminate coupling becomes increasingly efficient until at  $-78^{\circ}\text{C}$  only geminate coupling occurs.

The addition of free radical scavengers that are too large to enter the internal surface to the o-ACOB reaction system results in complete scrambling of the oA and B radicals (Figure 10). Importantly, addition of the same scavenger to the p-ACOB reaction system results in negligible scavenging of pA and B radicals.

Thus, the photolysis of o-ACOB and p-ACOB on ZSM zeolites allows a striking confirmation of the remarkable size/shape characteristics of zeolite molecule sieves in controlling chemical reactions of molecules adsorbed on the zeolite surface. The ability to control chemical reactivity via dynamics of molecular diffusion through channel systems of zeolites has been termed "molecular traffic control" of chemical reactions.<sup>13</sup>

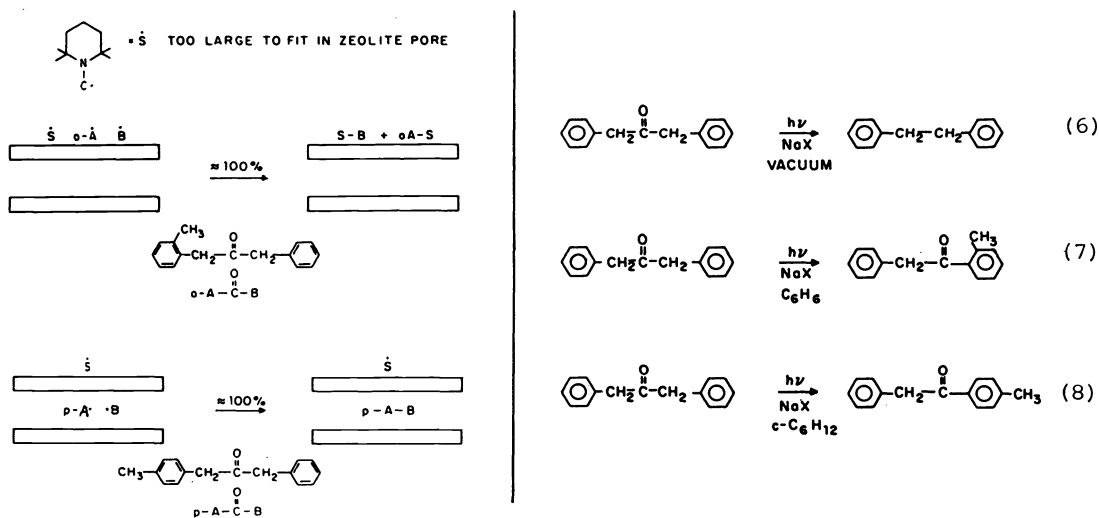


Figure 10. Radical scavenging of o-ACOB and p-ACOB. The free radical  $\dot{S}$  is too large to enter the internal ZSM surface. Co-adsorption of this scavenger does not result in radical trapping in the case of p-ACOB, but results in nearly quantitative trapping in the case of o-ACOB.

### Size and shape characteristics of X zeolites. A remarkable effect of additives

The 8Å diameter of the windows of X zeolites that leads to the supercages is large enough to allow ready diffusion of DBK molecules into the supercages. The diffusional characteristics of organic molecules adsorbed on NaX have been extensively studied because of the importance of this zeolite and of related zeolites as catalytic materials.<sup>14</sup> In general, the diffusion of adsorbed molecules becomes impeded as more molecules are added to the surface, i.e., as the surface coverage is increased.<sup>15</sup> This result is attributed to the increasing interference to diffusion of molecules due to the occupancy of the windows leading to the supercages and of the supercages themselves.

Once inside the supercages, DBK molecules would enjoy considerable diffusional freedom. Indeed, photolysis of DBK adsorbed on NaX (under vacuum, i.e., in the absence of air) results in formation of 1,2-diphenylethane (DPE) as the major product (eqn.6), a result analogous to that obtained in homogeneous solution. However, a striking change in the product composition is observed when simple molecules are coadsorbed on the NaX from the vapor phase so that the samples remain dry macroscopically.<sup>16</sup> For example, coadsorption of benzene with DBK on the NaX surface results in the formation of an isomeric DBK as the major photolysis product (eqn. 7)! The addition of cyclohexane as coadsorbed material results in the formation of a different isomeric DBK as the major product (eqn. 8).

The formation of DBK isomers as major products, rather than loss of CO when organic additives are coadsorbed with DBK, suggests that the additives are causing "congestion" of the space in the NaX supercage. This congestion inhibits diffusion of the primary geminate radical pair, and encourages reaction of the primary radical pair relative to the competing decarbonylation pathway. Figures 11 and 12 show schematically a mechanism consistent with the results. In the absence of additives, the primary geminate radical pair (A-C-B) is produced in a triplet state, and the diffusion of the pair into and out of the supercages is relatively unhindered so that separation of the pair occurs efficiently, and the separated radicals undergo efficient decarbonylation (Figure 11). The situation is similar to that for the photolysis of DBK in homogeneous solution. Indeed, measurement of the cage effect for substituted DBK's shows that only a small cage effect is observed under these conditions.

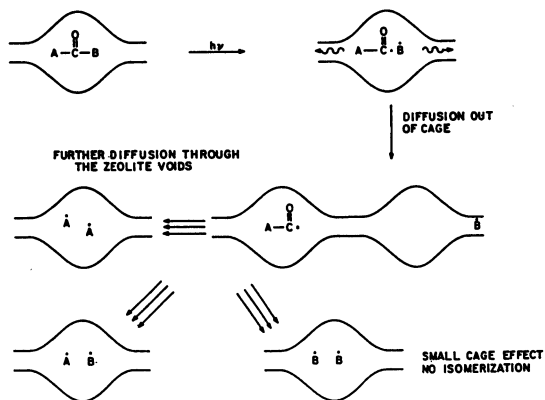


Figure 11. Schematic mechanism for the photolysis of DBK and substituted DBK's at low coverage in NaX. Diffusional separation is faster than primary geminate pair reactions. Decarbonylation occurs often after diffusional separation producing random radicals which eventually diffuse back together to yield a nearly statistical mixture of coupling products.

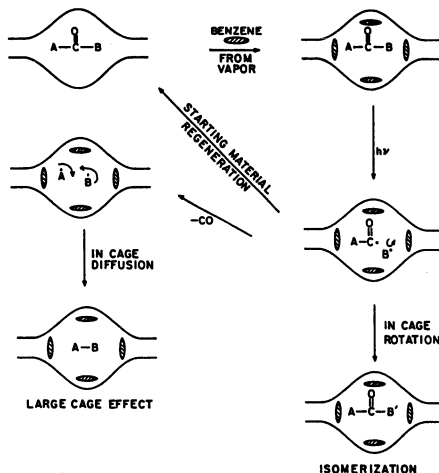


Figure 12. Schematic mechanism for the photolysis of DBK and substituted DBK's at low coverage on NaX. Diffusional separation is inhibited because of the congestion imposed by benzene coadsorbed in the supercages. See text for discussion.

Upon addition of benzene or cyclohexane vapor to the NaX system containing DBK, the additives are postulated to fill up the remaining void space in the supercage cavities. The additives thus tend to serve as a thin layer of molecular "solvent" molecules surrounding DBK in the supercage. This postulate is consistent with NMR investigations of benzene adsorbed on NaX<sup>17</sup> which lead to the conclusion that 5 or 6 benzene molecules can be included in each supercage and that benzene diffusion is very slow when the interior surface is saturated with benzene molecules. The benzene molecules cause congestion of the available void space and restrict the diffusional and rotational motion of the primary radical pairs produced by photolysis of DBK. As a result, recombination of the primary radical pairs is encouraged relative to the situation in the absence of benzene, and isomerization by coupling of the primary radical pair becomes competitive or favored relative to diffusional separation or decarbonylation (Figure 12). If decarbonylation does occur in competition with isomerization, the geminate benzyl radical pairs produced will face the congestive conditions and will have their diffusional separation retarded. The efficiency of cage recombination of these secondary radical pairs is expected to increase when benzene is added relative to vacuum, an expectation that is consistent with experiment.

### Mechanism of photolysis of isomerization of DBK adsorbed on NaX

A proposed mechanism for formation of the isomeric DBK's is shown in Figure 13. The primary geminate triplet radical pair is compelled by congestion within the supercage to undergo self-reaction rather than diffusion and decarbonylation. Radical coupling may occur to regenerate DBK itself. Since this would regenerate the starting material, it would not be observed in normal product analysis. However, <sup>13</sup>C enrichment studies would provide information on this point. Coupling of the acyl radical to the benzene ring of the benzyl radical would lead to an isomeric ketone as shown in Figure 13. An intermediate expected, but not

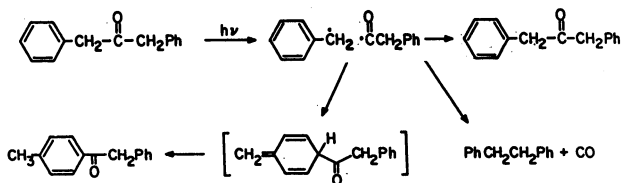


Figure 13. Proposed mechanism for formation of isomeric ketones from photolysis of DBK on NaX.



yet isolated, is the species produced by this first addition step (Figure 13). The isolated products are produced by a hydrogen transfer which achieves aromatization and produces the observed products.

It is interesting to speculate whether the photoisomerization could be achieved twice by a two photon process. If this occurred, DBK would be turned "inside out" and would produce a benzophenone product. Indeed, it was found that the photolysis of DBI on NaY, a zeolite which possesses the same internal surface topology as NaX, but which possesses a higher Si/Al ratio, produces a benzophenone as the major product.<sup>16</sup>

### Photolysis of large right cyclophanes adsorbed on NaX zeolites. Encarceration of products by ship in bottle and reptation mechanisms

The photolysis of small ring 2-phenyl cycloanones has been shown to result in the formation of enals as the major products (Figure 14).<sup>18</sup> No evidence for coupling of the primary radical pair to produce an isomeric ketone has been reported. If such a coupling occurred analogous to the photoisomerization of DBK observed on NaX, a cyclophane product would be produced ( $C_n$ , Figure 14). The size and shape of a cyclophane structure is quite distinct from that of the precursor cycloanone. In fact, from molecular models it is expected that for 12 carbon cyclanones the product, cyclophane, if formed in a supercage, could not exit because its size exceeds that of the window to allow exit from the supercage. These considerations suggested to us a "ship in bottle" strategy for encarceration of product molecules in a supercage as a result of change in the size/shape characteristics which result upon going from the starting material to the product. If it is true that the adsorbed starting cyclanone has a smaller size than the cyclophane, and if the cyclophane is produced in a supercage, then the product of a photochemical reaction would be encarcerated within the zeolite internal surface.

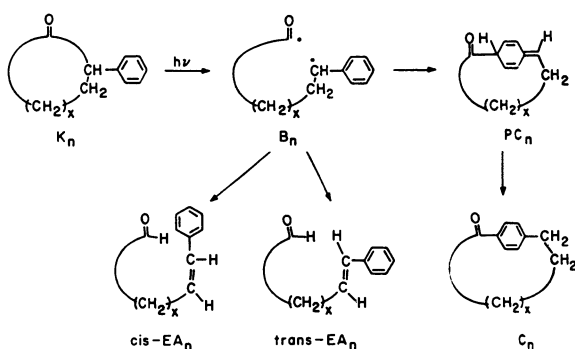


Figure 14. Mechanism for formation of products from photolysis of 2-phenylcycloanones,  $K_n$  ( $n$  = number of carbon atoms in a cyclanone ring). Absorption of light produces a biradical,  $B_n$ . The latter then either undergoes disproportionation to yield enals,  $EA_n$ , or cyclizes to form precyclophanes ( $PC_n$ ) which form cyclophanes ( $C_n$ ) by a hydrogen shift.

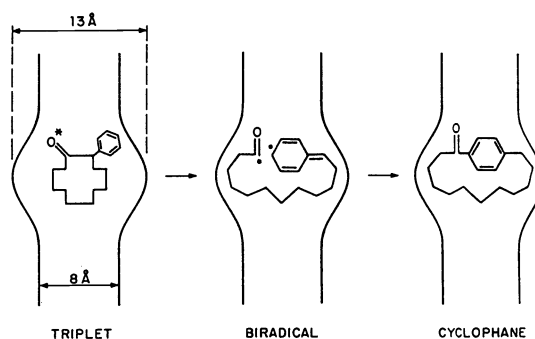


Figure 15. Suggested mechanism for the photolysis of 2-phenyl cyclododecanone adsorbed on NaX.

The experimental realization<sup>19</sup> of this strategy was achieved by the photolysis of 2-phenyl cyclododecanone adsorbed on NaX. This ketone is readily adsorbed on NaX from pentane solvent and readily extracted by benzene. This result means that the diffusion of the cyclanone to and out of the internal surface of NaX occurs without difficulty. It was observed that the photolysis of 2-phenyl cyclododecanone results in the disappearance of the starting material, but not in the appearance of significant amounts of extractable products, even when the photolysis was conducted to high conversions. It was discovered, however, that dissolution of the zeolite framework followed by extraction of products resulted in the isolation of a high yield of the cyclophane  $C_{12}$ .<sup>1</sup> From these results we suggest (Figure 15) that the cyclophane undergoes photochemical cleavage to form a biradical within the NaX supercage, that the resulting biradical undergoes a coupling reaction to produce the intermediate  $PC_{12}$  (Figure 14), and that the latter yields  $C_{12}$  after a hydrogen shift. Because of the larger size of the cyclophane, it is not capable of being extracted from the supercage by conventional solvent extraction. Thus, like a ship in bottle technique, an object that has a size and shape that is capable of passing through a window is converted to another object whose size and shape are sufficiently different to prevent reverse passage through the same window.

A second strategy for encarceration based on alteration of size and shape characteristics also occurred to us. If a cyclanone, which is too large initially to be adsorbed into the internal zeolite surface is photolyzed, the resulting biradical could gain access to the internal surface by slithering into and through the windows leading to the internal surface. Thus, entry to a supercage could be achieved by a "reptation" process. Once inside a supercage, cyclization to produce a cyclophane structure could occur, again leading to encarceration

of the product in the supercage. An experimental realization of this hypothetical possibility was achieved in the photolysis of 2-phenyl cyclopentadecanone adsorbed on Ca<sup>2+</sup> exchanged NaX. It was found that the cyclanone in this case was only weakly adsorbed, and could both be deposited and extracted with pentane solvent. These results are very analogous to those observed for the adsorption of o-ACOB on ZSM zeolites (*vide supra*.) In the latter case it was concluded that the o-ACOB was adsorbed only on the external zeolite surface. A similar conclusion is suggested here. Photolysis of the externally adsorbed cyclanone resulted in the disappearance of the starting material, but not the appearance of significant amounts of extractable products. It was discovered, however, that the dissolution of the entire zeolite framework with dilute hydrochloric acid, followed by product extraction, resulted in obtaining a high yield of the cyclophane C<sub>15</sub>! From these results we conclude that photolysis of the externally adsorbed ketone produces an externally adsorbed biradical which rapidly reptates into the internal zeolite framework, enters a supercage void, and then "backbites" itself to produce a cyclophane structure whose size and shape characteristics prevent escape from the supercage.

## CONCLUSION

The research described in this report attempted to capture the spirit of a method of investigation of photoreactions which, on the one hand takes advantage of well established photochemical systems to probe the structure of novel environments or "microscopic reactors" for the execution of photochemistry, and on the other hand takes advantage of the information concerning the structures of novel environments to develop new photoreactions. The next step in the process is to let an interaction between the photochemistry and the novel environment provide new insights to each system. The basic idea was to produce a geminate triplet radical pair or biradical from a substrate adsorbed on a zeolite surface. Simple product analyses allow the determination of geminate radical pair combination efficiency (i.e., the extent of the cage effect) and the ability of the zeolite surface to control reaction channels available to the primary geminate radical pair and subsequent radical pairs (i.e., the extent of formation and structure of isomeric ketones). The results allow conclusions to be made concerning the size/shape selectivity features of zeolite molecular sieves on photochemical reactions. This information should also be useful in adding to our knowledge of the mechanism of catalytic processes which occur on zeolites, since diffusion and size/shape selectivity are hallmark features of these catalytic materials.<sup>20</sup>

## Acknowledgements

The author gratefully acknowledges the financial support of this research by the National Science Foundation and the Department of Energy. He also acknowledges with pleasure the important scientific and intellectual contributions of his collaborators in various aspects of this research: Mr. Xuegong Lei, Dr. Peter Wan, and Dr. Chen-chih Cheng for developing and perfecting photochemical methods with zeolite substrates and for exceptional experimental execution of the experiments described in this report; Dr. Charles E. Doubleday, Jr. for initiating the investigation of 2-phenylcyclanones and for providing penetrating insight to the behavior of biradicals; Dr. Edith Flanigen of the Union Carbide Research Laboratory for her splendid tutorials on the delights of zeolite chemistry and for supplying samples of NaX; Dr. Lloyd Abrams and Dr. David Corbin of the Central Research Department of duPont Company for their excellent full collaborative contributions to the investigation of the ZSM class of zeolites.

## REFERENCES

1. A.F. Cronstedt, *K. Vetensk. Acad. Handl.* **17**, 120(1756).
2. Reviews of zeolites: (a) E.G. Derouane, *Intercalation Chemistry*, eds. M.S. Whittingham and A.J. Jacobson, Academic Press, p. 101, Academic Press, New York (1982); (b) D.W. Breck, *Zeolite Molecular Sieves*, Wiley, New York 1974; (c) *Natural Zeolites: Occurrence, Properties, Use*, eds. L.B. Sandard and F.A. Mumpton, Pergamon Press, Oxford (1978).
3. D.B. Tagiev and K.M. Minachev, *Russ. Chem. Rev.* **50**, 1929 (1981) and references therein.
4. E.C. Derouane, *Zeolites: Science and Technology*, eds. F.R. Ribeiro, p. 515, Nyhoff, the Hague (1984).
5. N.J. Turro, *Modern Molecular Photochemistry*, p. 528, Benjamin/Cummings, Menlo Park, CA. 1978.
6. *ibid.*, p. 386.
7. N.J. Turro and P. Wan, *Tetrahedron Letters*, 3655 (1984).
8. H.L. Casal and J.C. Scaiano, *Can. J. Chem.* **62**, 628 (1984);
9. (a) P.S. Engel, *J. Am. Chem. Soc.* **92**, 6074 (1970); (b) W.K. Robbins and R.H. Eastman *ibid.*, **92**, 6076, 6-77 (1970).
10. N.J. Turro, *Acc. Chem. Res.* **13**, 369 (1980).
11. N.J. Turro, X. Lei, C.C. Cheng, D.R. Corbin, and L. Abrams, *J. Am. Chem. Soc.* **107**, 5824 (1985).
12. (a) N.J. Turro, I.R. Gould, and B.H. Baretz, *J. Phys. Chem.* **87**, 531 (1983); (b) L. Lunazzi, K.U. Ingold, and J.C. Scaiano, *J. Phys. Chem.* **87**, 549 (1983).
13. J.B. Nagy, E.G. Derouane, H.A. Resing, and G.R. Miller, *J. Phys. Chem.* **87**, 833 (1983).
14. P.B. Weisz and V.J. Friblette, *J. Phys. Chem.* **64**, 382 (1960).
15. D.M. Ruthven, *Principles of Adsorption and Adsorption Processes*, Wiley, New York (1984).
16. N.J. Turro, C.C. Cheng, X. Lei, and E.M. Flanigen, *J. Am. Chem. Soc.* **107**, 3740 (1985); N.J. Turro and P. Wan, *ibid.* **107**, 678 (1985).
17. H. Pfeifer, W. Schirmer, and H. Winkler, in *Molecular Sieves*, eds. W. Meier and J.B. Uytterhoven, *Adv. Chem. Ser. ACS*, no. 121, p. 430 (1973).
18. P.J. Wagner and T. Stratton, *Tetrahedron*, **37**, 3317 (1981); A.A. Baum, *Tetrahedron Letters*, 1817 (1972).
19. X. Lei, C.E. Doubleday, Jr., M.B. Zimmt, and N.J. Turro, *J. Am. Chem. Soc.* **108**, 2444 (1986).
20. P.B. Weisz, *Ind. Eng. Fund.* **25**, 53 (1986).